An Endogenous Sulfated Inhibitor of Neuronal Inositol Trisphosphate Receptors†

James Watras,*,‡ Ron Orlando,§ and Ion I. Moraru‖

Departments of Medicine and Surgery, University of Connecticut Health Center, Farmington, Connecticut 06030, and Complex Carbohydrate Research Center and the Department of Biochemistry and Molecular Biology, University of Georgia, Athens, Georgia 30602-4712

Received September 20, 1999; Revised Manuscript Received December 21, 1999

ABSTRACT: In cerebellum, inositol trisphosphate- ($InsP_3$-) gated Ca channels play a key role in learning, though they exhibit a low sensitivity to $InsP_3$ compared to peripheral tissues. In the present study, the cerebellar $InsP_3$ receptor is shown to be associated with a novel inhibitor of $InsP_3$ binding. ^{3}H-$InsP_3$ binding studies indicated that this inositol trisphosphate receptor inhibitor (IRI) could completely inhibit $InsP_3$ binding to the purified cerebellar $InsP_3$ receptor and acted as a competitive inhibitor. Gel filtration of IRI showed a predominant peak at 6500 Da, though this peak appeared to be an aggregate (with a monomeric molecular mass of approximately 1500 Da). Mass spectrometry of IRI showed a predominant peak at 1635 *m*/*z*, consistent with this low molecular mass estimate. The inhibitory activity of IRI was prevented by pretreatment with aryl sulfatase, suggesting the presence of a critical sulfo ester in IRI. IRI was insensitive to proteases and organic extraction but bound to concanavalin A, suggesting that IRI is a sulfated glycan. IRI was present in cerebellum but below the level of detection in aorta. IRI was also present in the neuronal cell line N1E115 (which exhibits a low sensitivity to $InsP_3$). We conclude that IRI is a novel endogenous sulfated inhibitor of the $InsP_3$ receptor that modulates the sensitivity of the $InsP_3$ receptor and thus may explain the low $InsP_3$ sensitivity of neurons.

Inositol 1,4,5-trisphosphate ($InsP_3$)[1] receptors are found in virtually all cell types (*1*−*3*) and play a critical role in elevation of intracellular calcium (Ca) in the presence of various hormones or neurotransmitters (*4*, *5*). In the cerebellar Purkinje cell, $InsP_3$-gated Ca channels are involved in the development of long-term depression (*6*−*8*), important for learning (*9*). The concentration of $InsP_3$ needed to activate the $InsP_3$-gated Ca channel in cerebellar Purkinje cells, however, is 50 times higher than that needed for a variety of nonneuronal cells (*10*−*12*) or from purified cerebellar microsomes (*13*). This low $InsP_3$ sensitivity has also been observed in differentiated neuroblastoma cells (*14*), suggesting that it may be a general property of neurons.

The mechanism underlying this low $InsP_3$ sensitivity of the cerebellar Purkinje cell is unclear, but it does not appear to be an intrinsic property of the $InsP_3$ receptor. That is, the isolated/purified cerebellar $InsP_3$ receptor exhibits a high sensitivity to $InsP_3$ (*15*−*17*), comparable to that seen in peripheral tissues (*18*). Moreover, cerebellar microsomes exhibit a high sensitivity of $InsP_3$-gated channel activity (*13*), comparable to that seen in peripheral tissues. This raises the possibility that cerebellar Purkinje cells contain an endogenous inhibitor of $InsP_3$ binding.

Recently, it was reported that calmodulin acts as an inhibitor of $InsP_3$ binding independent of Ca concentration, raising the possibility that high concentrations of calmodulin in the brain may contribute to this low sensitivity to $InsP_3$ in Purkinje cells in vivo (*19*). Calmodulin binding sites are known to exist on the cerebellar $InsP_3$ receptor (*20*), and recent studies indicate that calmodulin may contribute to the Ca-dependent feedback inhibition of channel activity at Ca concentrations in excess of 0.3 μM (*21*−*23*). The possibility that calmodulin contributes to the decreased $InsP_3$ affinity at resting intracellular Ca concentrations, however, is controversial, and in fact our data suggest that calmodulin is a weak inhibitor of $InsP_3$ binding at low Ca concentrations (see Results).

In the present study, we show that cerebellum contains a novel $InsP_3$ receptor inhibitor (IRI) and provide evidence that IRI is present in neuronal cells that exhibit a low $InsP_3$ sensitivity. Binding studies show that IRI acts as a competitive inhibitor. Structural insights into the identity of IRI are also provided, along with the elucidation of functional groups critical for the inhibitory activity of IRI. A preliminary report of this study has been presented (*24*).

EXPERIMENTAL PROCEDURES

Isolation of IRI. Initially, IRI was isolated from cerebellar microsomes by detergent solubilization, followed by hep-

† Supported by National Institutes of Health Grants RR13186 (J.W. and I.I.M.) and 2-P41-RR05351 (R.O.) and by a grant from the University of Connecticut Health Center (J.W.).

* Address correspondence to this author at the Department of Physiology, MC3505, University of Connecticut Health Center, Farmington, CT 06032. Tel 860-679-2896; fax 860-679-1269; email watras@sun.uchc.edu.

‡ Department of Medicine, University of Connecticut Health Center.

§ University of Georgia.

‖ Department of Surgery, University of Connecticut Health Center.

[1] Abbreviations: $InsP_3$, inositol 1,4,5-trisphosphate; Ca, calcium; DTT, dithiothreitol; EDTA, ethylenedinitrilotetraacetic acid; EGTA, ethylene glycol bis(β-aminoethyl ether)-*N*,*N*,*N*′,*N*′-tetraacetic acid; Tris, tris(hydroxymethyl)aminomethane; HEPES, *N*-(2-hydroxyethyl)piperazine-*N*′-2-ethanesulfonic acid; PMSF, phenylmethanesulfonyl fluoride; PEG, poly(ethylene glycol); TCA, trichloroacetic acid; conA, concanavalin A; MALDI-TOF MS, matrix-assisted laser desorption/ionization time-of-flight mass spectrometry; PIP_2, phosphatidylinositol 4,5-bisphosphate; IRI, inositol 1,4,5-trisphosphate receptor inhibitor.

10.1021/bi992175v CCC: $19.00
Published on Web 02/29/2000

arin−Sepharose chromatography and gel filtration. The heparin−Sepharose chromatography provided a convenient means of separating IRI from the $InsP_3$ receptor. For these initial studies, cerebellar microsomes were isolated from canine cerebellum by differential centrifugation (as described previously) (*13*) and then solubilized (2 mg/mL) in buffer A (1 mM DTT, 1 mM EDTA, and 50 mM Tris, pH 8, 30 min, 0 °C) with 1.5% Triton X-100 and protease inhibitors (10 μg/mL pepstatin A, 10 μg/mL leupeptin, 10 μg/mL aprotinin, and 1 mM PMSF). The detergent-solubilized preparation was centrifuged at 100000*g* for 1 h (4 °C) and then subjected to heparin−Sepharose chromatography. The column was equilibrated with buffer A containing 0.1% Triton X-100 and 0.25 M NaCl, such that the $InsP_3$ receptor bound to the column, whereas the inhibitor (IRI) passed through in the unretained fraction. The latter fraction was concentrated (by lyophilization) and subjected to gel filtration (Superose 12). All column fractions were assayed for ability to inhibit ^{3}H-$InsP_3$ binding to the purified cerebellar $InsP_3$ receptor, as described below.

Subsequently, a four-step procedure for purifying IRI was developed, without the need for detergent solubilization. Specifically, cerebellar microsomes (10 mg) were subjected to Folch extraction (*25*), and then the aqueous phase of the Folch extract was dried under a stream of nitrogen and resuspended in 300 μL of gel-filtration buffer (20 mM Tris and 150 mM NaCl, pH 7.6). The latter preparation was filtered (0.2 μm), deaerated, and then subjected to gel filtration (10 × 20 Sepharose 12 column; 200 μL sample volume, 0.5 mL/min flow rate, 0.75 mL/fraction). Column fractions were assayed for inhibition of ^{3}H-$InsP_3$ binding to purified $InsP_3$ receptor (as described below). Peak inhibitory fractions were lyophilized, resuspended in 250 μL of water, and resubjected to gel filtration (Sepharose 12, equilibrated with 50 mM Tris, pH 8). Peak inhibitory fractions from the latter gel filtration were applied to a MonoQ anion-exchange column, and eluted with a linear gradient with ammonium formate (0.2−1.7 M). Fractions from the MonoQ column were subjected to three rounds of lyophilization and resuspension in water (to ensure removal of the volatile buffer), and then fractions were assayed for inhibitory activity (as described below).

Protein concentration in the various fractions was determined with a protein assay kit (Bio-Rad Laboratories; *26*), with bovine serum albumin as a standard. Carbohydrate content of IRI in various fractions was determined with a glycoprotein carbohydrate estimation kit (Pierce, Rockford, IL), with glucose as a standard.

^{3}H-$InsP_3$ Binding. The purification of IRI was monitored by assessing the ability of isolated fractions to inhibit ^{3}H-$InsP_3$ binding to purified canine cerebellar $InsP_3$ receptor. Specifically, 5 μL of a given column fraction was added to ^{3}H-$InsP_3$ binding medium (which contained buffer A with 50 mM NaCl, 5 nM ^{3}H-$InsP_3$, 100 μg of rabbit γ-globulin, and 1 μg of purified cerebellar $InsP_3$ receptor). Following a 5 min incubation (0 °C) in the specified ^{3}H-$InsP_3$ binding medium, reactions were terminated by poly(ethylene glycol) (PEG) precipitation, and the pellet was assayed for radioactivity, as described previously (*27*). Control and nonspecific binding were determined by including a 5 μL aliquot of gel-filtration buffer without or with 1 mg/mL heparin in the binding assay, respectively.

To quantitate the activity of IRI at each stage of the purification, a standard assay was developed. One inhibitory unit was defined as the amount of IRI needed to produce a 50% inhibition of $InsP_3$ binding under standard conditions (described above). Curve-fitting analyses were used to calculate the volume of IRI needed for one inhibitory unit in a given fraction. This value was then divided into the total volume of a given fraction to yield the total number of inhibitory units in the fraction.

The $InsP_3$ receptor preparations used in these screening assays were obtained from canine cerebellar microsomes. Briefly, cerebellar microsomes (2 mg/mL) were solubilized as described above, and then the supernatant was applied to a heparin−Sepharose column equilibrated with buffer A containing 0.25 M NaCl and 0.1% Triton X-100. The $InsP_3$ receptor was eluted from this column at 0.5 M NaCl.

Reversibility of IRI Inhibition of $InsP_3$ Binding. Cerebellar microsomes (3 μg) were preincubated in buffer B (3 mM $NaHCO_3$, 0.3 mM EGTA, and 0.3 mM EDTA, pH 7.0, 0 °C) for 8 min in the absence or presence of 2 μL of IRI, and then the samples were centrifuted (40000*g*, 10 min, 2 °C) and the pellets were assayed for $InsP_3$ binding level (in buffer A with 5 nM ^{3}H-$InsP_3$). Results from the latter experiments indicated that exogenously added IRI cosedimented with the cerebellar microsomes under this condition. To assess the reversibility of the apparent association/cosedimentation of exogenously added IRI with the cerebellar microsomes, the preincubation buffer described above (containing 3 μg of cerebellar microsomes with and without 2 μL of IRI) was diluted with one volume of buffer B or buffer C (1.2 M KCl, 40 mM $Na_4P_2O_7$, 10 mM NaN_3, and 20 mM HEPES, pH 7.2, 0 °C), followed by centrifugation and then assaying the pellet for $InsP_3$ binding (in buffer A with 5 nM ^{3}H-$InsP_3$).

Sulfatase Treatment of IRI. The effects of aryl sulfatase (EC 3.1.6.1) on the inhibitory activity of IRI were determined by pretreating a submaximal concentration of purified IRI with 3.2 milliunits/μL aryl sulfatase for 2 h (37 °C). The sulfatase reactions were terminated by boiling (2 min), followed by centrifugation (2000*g*, 1 min). An aliquot (5 μL) of the supernatant fluid was assayed for ability to inhibit $InsP_3$ binding to the purified cerebellar $InsP_3$ receptor (as described above). Controls included (1) buffer (without IRI), (2) the specified sulfatase without IRI, and (3) IRI without sulfatase. Controls were subjected to the incubation (2 h, 37 °C), boiling, and centrifugation (identical to the sulfatase-treated samples).

Concanavalin A (conA) Binding. The 6500 Da fraction of IRI was incubated in 0.5 mL of buffer D (50 mM Tris, 1 mM $MgCl_2$, 1 mM $CaCl_2$, and 0.15 M NaCl, pH 7.4) in the presence of conA−Affi-Gel beads for 20 min at 4 °C and then centrifuged at 2000*g* for 30 s. Aliquots of supernatant were assayed for ability to inhibit ^{3}H-$InsP_3$ binding to the purified cerebellar $InsP_3$ receptor. Dilution of IRI in the conA beads was subsequently determined by addition of ^{3}H-inulin to the tubes containing conA beads.

Reductive Amination and Fluorescent Labeling. Heparin, IRI, and dextran (10 kDa) were subjected to reductive amination, followed by incubation with the fluorescent label 2-aminobenzoic acid (using the Signal 2AA fluorescent labeling kit from Glyko, Inc., Novato, CA). Fluorescent label-treated samples were lyophilized, resuspended in gel-filtration buffer, and then subjected to gel filtration (Superose 12

column; 20 mM Tris and 150 mM NaCl, pH 7.6). Gel-filtration fractions were assayed for fluorescence (Hitachi F2000 spectrofluorometer; excitation 330 nm; emission 420 nm) and the ability to inhibit ^{3}H-InsP_3 binding to purified cerebellar InsP_3 receptor (as described above).

MALDI-TOF Measurements. Mass spectra of IRI were obtained on a Kratos SEQ MALDI-TOF mass spectrometer. This instrument was operated to detect negatively charged ions in linear mode using pulsed ion extraction that was optimized for ions with a *m*/*z* of 1600, with an accelerating voltage of −20 kV and a pressure below 1×10^{-6} Torr. The samples were desorbed/ionized from the probe tip by use of a nitrogen laser source with an output wavelength of 337 nm. Calibration was performed with mixtures of peptides with known molecular masses. α-Cyano-4-hydroxycinnamic acid dissolved in 70% aqueous acetonitrile with 0.01% trifluoroacetic acid was used as the MALDI matrix for experiments performed on the Kratos instrument.

N1E115 Cells. Differentiated N1E115 neuroblastoma cells were grown as described previously (*28*). The intracellular volume was determined by a combination of ^{3}H-inulin and ^{14}C-urea radiochemical techniques, and shown to be 2.5 μL/mg of total protein (*14*). For the quantification of IRI in N1E115 cells, the cells were washed (by gentle resuspension/centrifugation) three times in Earle's balanced salt solution (pH 7.2), and then the pellet was subjected to Folch extraction (following brief sonication). An aliquot of the homogenate/sonicate was assayed for protein concentration (for the purpose of calculating the total amount of protein and intracellular water subjected to Folch extraction).

Comparison of IRI with Known Inhibitors of the InsP_3 Receptor. The inhibition of InsP_3 binding to purified cerebellar InsP_3 receptor by PIP_2 (10 nM) and calmodulin (10 μM) was assessed under standard assay conditions described above (pH 8). When specified, the effect of calmodulin (3−20 μM) and IRI (2 μL) on InsP_3 binding to purified cerebellar InsP_3 receptor was also examined at pH 7 (70 mM KCl, 1 mM EGTA, 20 mM HEPES, and 5 nM ^{3}H-InsP_3, 0 °C).

RESULTS

Isolation of IRI from Cerebellar Microsomes. From detergent-solubilized cerebellar microsomes, an inhibitor of InsP_3 binding was separated from the InsP_3 receptor by heparin-affinity chromatography (Figure 1). This inhibitor preparation decreased InsP_3 binding to the purified InsP_3 receptor in a concentration-dependent manner (Figure 1A), due to a decrease in InsP_3 binding affinity (Figure 1B). The inhibitor was further purified by gel filtration and yielded peak inhibitory activity in fraction 16 (Figure 1C; ca. 6500 Da), with a second (lesser) inhibitory peak in fractions 20−21 (Figure 1C; ca. 1500 Da). There was little protein in the predominant inhibitory peak (fraction 16), as evidenced by the absorbance data (280 nm; dashed line in Figure 1C). When fraction 16 was reapplied to the Superose 12 column, inhibitory peaks were observed in both fraction 16 (ca. 6500 Da) and fraction 20 (ca. 1500 Da), suggesting that these two inhibitory peaks are related. We hypothesize that the 6500 Da inhibitory peak may be an aggregate (e.g., tetramer) of the 1500 Da inhibitor.

The above data indicate that a low molecular weight inhibitor of InsP_3 binding can be separated from the InsP_3 receptor by a technique commonly employed for InsP_3 receptor preparation (viz., solubilization in Triton X-100, followed by heparin-affinity chromatography).

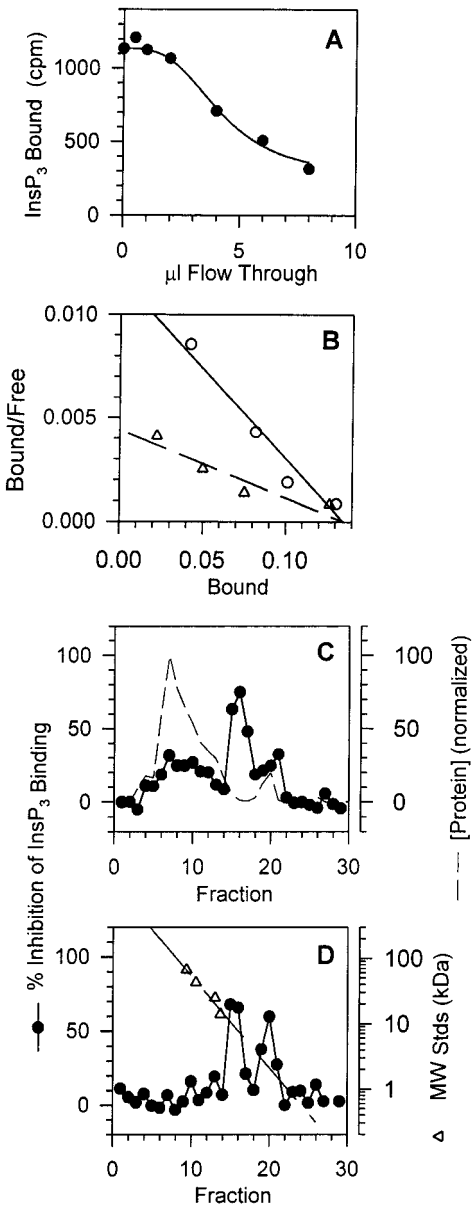

FIGURE 1: Isolation of an inhibitor of the InsP_3 receptor from detergent-solubilized cerebellar microsomes. The inhibitor (which was separated from detergent-solubilized cerebellar InsP_3 receptor by heparin−Sepharose chromatography) decreased InsP_3 binding to purified cerebellar InsP_3 receptor in a concentration-dependent manner (panel A). This decrease in InsP_3 binding was attributable to an increase in the K_D for InsP_3 binding (panel B). The K_D for InsP_3 binding to the purified cerebellar InsP_3 receptor increased from 12 nM in the absence of inhibitor (○) to 50 nM in the presence of 3 μL of inhibitor (△). The inhibitor was further purified by gel filtration, with peak activity in fraction 16 (●, panel C; predicted molecular mass = 6500 Da). The dashed line in panel C represents absorbance at 280 nm and indicates that there is very little (if any) protein in this fraction. A second inhibitory peak was present in fractions 20−21 (panel C). Reapplication of fraction 16 to the gel-filtration column yielded a similar profile, with inhibitory peaks in fractions 16 (6500 Da) and 20 (1500 Da) (panel D), suggesting that the 6500 Da inhibitor may be an aggregate of the 1500 Da inhibitor. The dashed line (△) in panel D represents the molecular weight calibration.

The inhibitor was resistant to organic extraction, partitioning into the aqueous phase with either the Folch technique (*25*) or the Bligh and Dyer technique (*29*). The resistance

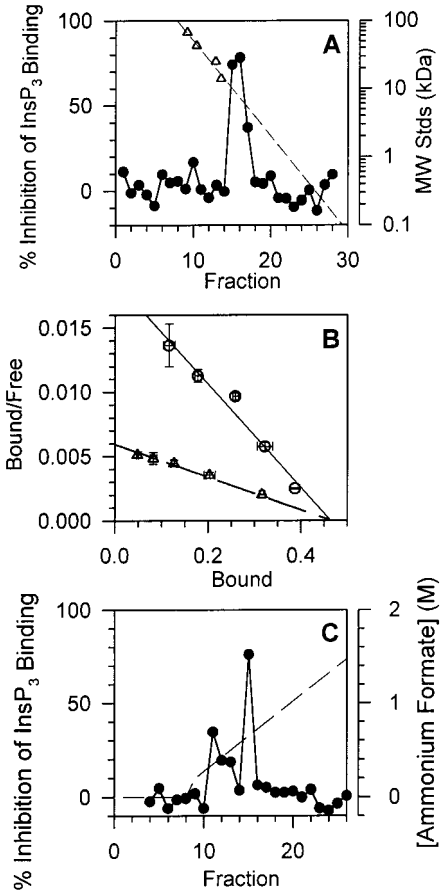

FIGURE 2: Purification of the $InsP_3$ receptor inhibitor (IRI) in the absence of detergent. Cerebellar microsomes were first subjected to organic extraction and then the aqueous phase was applied to a gel-filtration column, yielding peak inhibitory activity in fraction 16 (panel A). The dashed line and unfilled triangles in panel A represent the molecular weight calibration, with fraction 16 exhibiting a predicted molecular weight of 6500 Da. Panel B shows that fraction 16 increased the K_D for $InsP_3$ binding. Data in panel B represent mean ± SE ($n = 3$) for $InsP_3$ binding to the purified cerebellar $InsP_3$ receptor in the presence (△) or absence (○) of 1 μL of fraction 16 from panel A. Fraction 16 from panel A was subjected to a second gel filtration (in the absence of salt), followed by anion-exchange chromatography. Panel C shows the anion-exchange elution profile (with peak activity eluting at 0.65 M ammonium formate; fraction 15).

of the inhibitor to organic extraction proved useful as an initial purification step, since it avoided the need for detergent and removed both lipids and the bulk of the protein from the microsomal preparation. That is, lipids were extracted into the organic phase, whereas 95% of the protein was denatured (concentrating at the interface of the organic and aqueous phases). The aqueous phase (containing the inhibitor) was subjected to gel filtration, and as shown in Figure 2A, it exhibited peak inhibitory activity in fraction 16 (ca. 6500 Da). The mechanism of inhibition of $InsP_3$ binding was attributed to an increase in the dissociation constant for $InsP_3$ binding (Figure 2B), consistent with results obtained for the detergent-solubilized, heparin-affinity-purified inhibitor (Figure 1B). Further purification of this $InsP_3$ receptor inhibitor (IRI) was accomplished by a second round of gel filtration (in the absence of salt), followed by anion-exchange chromatography. Peak inhibitory activity eluted from the anion exchange column at 0.65 M ammonium formate (fraction 15, Figure 2C).

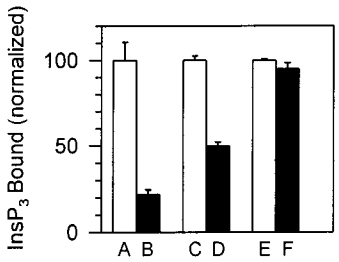

FIGURE 3: Reversibility of IRI inhibition of $InsP_3$ binding. $InsP_3$ binding to cerebellar microsomes was measured in the absence (A) and presence (B) of 2 μL of IRI. When cerebellar microsomes were preincubated in low ionic strength buffer in the absence (C) and presence (D) of 2 μL of IRI, followed by centrifugation, the pellet of the IRI-treated sample exhibited partial inhibition of $InsP_3$ binding (cf. C vs D). Bars E and F are identical to C and D, respectively, except that preincubation media were diluted with one volume of high ionic strength buffer before centrifugation, resulting in a reversal of the inhibition of the IRI-treated sample (F). Data represent mean ± SE for $n = 3$. See text for details.

Reversibility of IRI Inhibition of $InsP_3$ Binding. A high ionic strength buffer (typically used in the preparation of cerebellar microsomes) appears to promote the dissociation of IRI from cerebellar microsomes. As shown in Figure 3, 2 μL of IRI (B) resulted in an 80% inhibition of $InsP_3$ binding to cerebellar microsomes compared to the control (A). If the cerebellar microsomes are diluted in a low ionic strength buffer (3 mM $NaHCO_3$, 0.3 mM EGTA, and 0.3 mM EDTA, pH 7.2) in the absence (C) and presence (D) of 2 μL of IRI, and then centrifuged, the IRI-treated pellet (D) continues to exhibit partial inhibition of $InsP_3$ binding. This suggests that some of the IRI has cosedimented with the cerebellar microsomes in the presence of low ionic strength buffer. If, after preincubating the cerebellar microsomes in the above low ionic strength buffer in the absence (E) and presence (F) of 2 μL of IRI, the samples are further diluted in a high ionic strength buffer (resulting in a final concentration of 0.6 M KCl, 20 mM $Na_4P_2O_7$, 5 mM NaN_3, 10 mM HEPES, 1.5 mM $NaHCO_3$, 0.15 mM EGTA, and 0.15 mM EDTA, pH 7.2, 0 °C) and then centrifuged (40000*g*, 10 min), there is no longer an inhibition of $InsP_3$ binding in the pellet of the IRI-treated sample (F). Moreover, the $InsP_3$ binding level of the pellet from these IRI-treated samples (F) (1934 ± 73 cpm) was comparable to that seen in the other controls (A and C) (1937 ± 294 cpm), indicating that all of the microsomes containing $InsP_3$ binding sites had pelleted in the presence of both low ionic strength and high ionic strength buffer. These data suggest that high ionic strength buffer promotes the dissociation of IRI from cerebellar microsomes, so that IRI no longer cosediments with the cerebellar microsomes.

Elucidation of Functional Groups on IRI. The functional groups on IRI responsible for its inhibitory activity were elucidated through the use of sulfatases. As shown in Figure 4, the inhibitory effects of IRI were largely prevented by pretreatment of IRI with aryl sulfatase (EC 3.1.6.1), suggesting the presence of critical sulfo ester group(s) on IRI. Pretreatment of IRI with sulfamidase (EC 3.10.1.1), however, did not prevent the inhibitory activity of IRI (data not shown), suggesting that N-linked sulfates are not critical for the inhibitory activity of IRI. This contrasts with heparin, which has been reported to require the presence of N-linked sulfates for the inhibition of the $InsP_3$-gated Ca channel (*30*) and

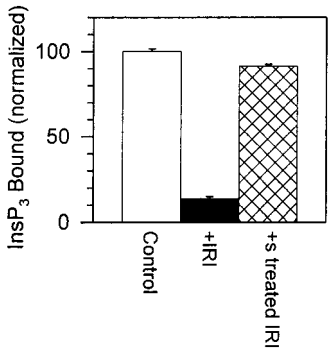

FIGURE 4: Inhibitory activity of IRI (solid bar) was reversed by pretreatment of IRI with aryl sulfatase (crosshatched bar). Data represent mean ± SE for $n = 4$. See text for details.

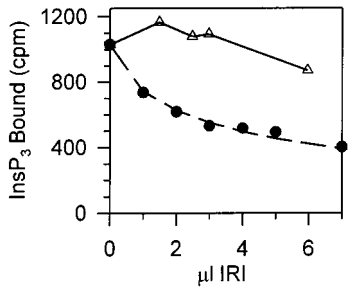

FIGURE 5: Inhibitory activity of IRI is precipitated by conA beads. (△) Inhibitory activity of a 6500 Da fraction of IRI after incubation/centrifugation with conA beads. Various volumes of the supernatant were assayed for ability to inhibit $InsP_3$ binding. (●) Inhibitory activity of equivalent amounts of the 6500 Da fraction of IRI (not treated with conA beads).

whose inhibitory activity persisted after treatment with aryl sulfatase (data not shown).

The inhibitory activity of IRI was also lost upon treatment with conA beads (Figure 5). Specifically, incubation of IRI with conA beads for 20 min, followed by centrifugation, effectively removed the inhibitory activity from the supernatant. The solid circles in Figure 5 represent the inhibitory activity of equivalent volumes of IRI solution treated identically to the conA samples, except for the omission of conA beads. These data suggest that IRI binds to conA and thus probably contains mannose residues.

The inhibitory activity of IRI was not blocked by treatment with trichloroacetic acid (TCA) (10−20%) or the proteases trypsin and subtilisin (data not shown). The gel-filtration profile of IRI was also unaffected by pretreatment with trypsin, suggesting that IRI is not a glycoprotein.

Preliminary thin-layer chromatography of IRI on silica gel 60 was also consistent with the presence of carbohydrate moieties in IRI, as a purified preparation of IRI stained green with orcinol and fluoresced with anisaldehyde. There was no detectable staining of purified IRI, however, by resorcinol (for sialic acids), rhodamine 6G and iodine vapor (for lipids), or ninhydrin (for protein). Moreover, there was no evidence of migration of IRI with the mobile phases chloroform/methanol (2:1) or chloroform/methanol/acetic acid/water (25:15:4:2), which are typically used for phospholipids and gangliosides. Instead, separation was achieved by use of the mobile phase *n*-propanol/28% NH_4OH/water (6:1:2.5), which is typically used for highly charged oligosaccharides.

To assess the possibility that IRI is a sulfated oligosaccharide, samples were assayed for the presence of a free

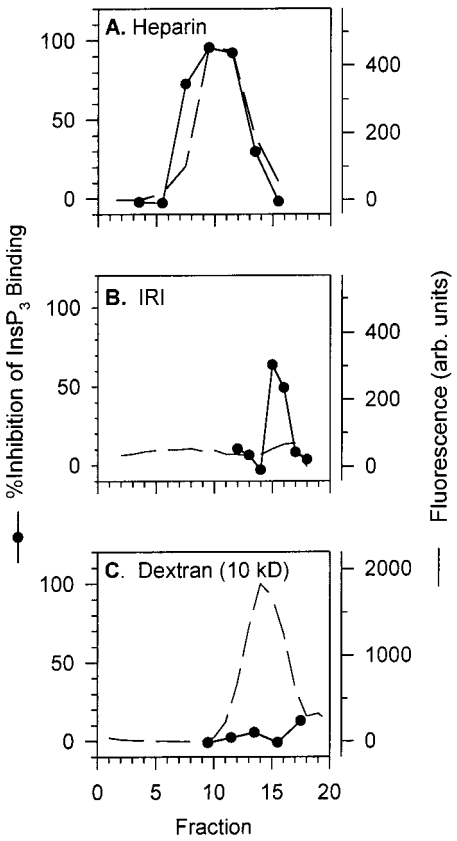

FIGURE 6: IRI lacks a free reducing terminus. Heparin (A), purified IRI (B), and dextran (10 kDa; C) were subjected to reductive amination, followed by fluorescent labeling (Signal 2AA kit; Glyko, Inc) and then gel filtration. Gel-filtration fractions were assayed for fluorescence (− − −) and ability to inhibit $InsP_3$ binding to purified $InsP_3$ receptor (●). IRI eluted in fractions 15−16 (B), as usual, with no detectable incorporation of fluorescent label, suggesting that IRI lacks a reducing terminus.

reducing terminus by using the fluorescent probe 2-aminobenzoic acid. Controls included heparin and dextran (10 kDa). All treated samples were subjected to gel filtration to separate the unreacted fluorophore from the labeled sample. The location of heparin and IRI in the column eluate was also assessed by analyzing column fractions for ability to inhibit $InsP_3$ binding to purified $InsP_3$ receptor. As shown in Figure 6A, the inhibitory peak for heparin-treated samples coincided with the fluorescent peak, indicating that heparin incorporated the fluorescent label (as expected, since heparin is a mucopolysaccharide with a free reducing terminus). The inhibitory peak for IRI, however, showed no evidence of fluorescent labeling, suggesting that IRI lacks a free reducing terminus (Figure 6B). Figure 6C shows the gel-filtration profile of noninhibitory control (10 kDa dextran), which clearly incorporated the fluorescent label but (as expected) showed no inhibition of $InsP_3$ binding. The high level of fluorescence of the labeled dextran (compared to heparin) was attributable to the presence of approximately three branches (and hence three reducing termini) in the dextran molecule (i.e., 95% α(1−6) linkages and 5% α(1−3) linkages; manufacturer's data sheet).

MALDI-MS Analyses of IRI. The MALDI-MS spectra of IRI purified from canine cerebellum is shown in Figure 7. A cluster of peaks was present in the range 1501−1688 *m*/*z*, with peak amplitude at 1635 *m*/*z*. The reason for the cluster is not clear, but it may in part reflect the formation of salt

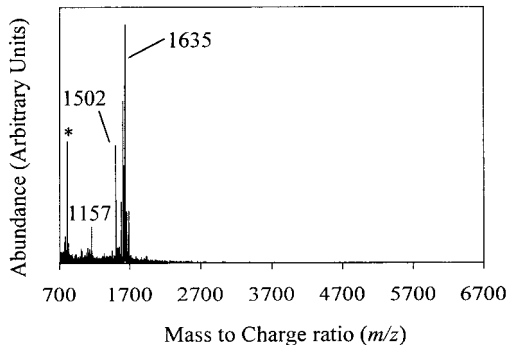

FIGURE 7: MALDI-TOF MS analysis of IRI. The peak eluate from the Mono Q column (0.65 M ammonium formate peak) was subjected to MALDI-TOF mass spectrometry. A cluster of peaks was observed in the range 1501−1688 *m*/*z*, with the greatest signal at 1635 *m*/*z*. The peak marked with an asterisk represents a matrix artifact.

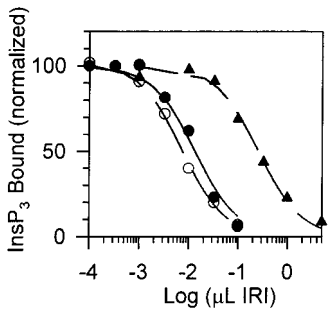

FIGURE 8: Quantification of IRI in canine cerebellum. One unit of IRI activity is defined as the amount of IRI solution needed to inhibit $InsP_3$ binding by 50%. Representative inhibition curves for cerebellar extract (aqueous phase of the Folch extract; ●), the peak inhibitory fraction from the first gel filtration (○), and the peak inhibitory fraction from the second gel filtration (▲) are shown. Total inhibitory activities shown in Table 1 were obtained by dividing the total volume of an inhibitory peak by the volume needed to yield half-maximal inhibition of $InsP_3$ binding.

adducts and/or partial fragmentation of IRI. The peak at 1157 *m*/*z* appears to be a fragment, as its amplitude increased when conditions were used to promote fragmentation. These peaks were not present in any of the controls, using noninhibitory fractions from the MonoQ column. The peak at 808 *m*/*z* (marked with an asterisk in Figure 7) represents a matrix artifact. The predominant mass of IRI shown in Figure 7 (1635 *m*/*z*) is consistent with the predicted monomeric molecular mass of IRI following gel filtration (1500 Da; cf. Figure 1D). It should be noted that the spectrum shown in Figure 7 was obtained when MALDI-MS was run in negative-ion mode, whereas no peaks were observed when IRI was run in positive-ion mode. This result suggests that IRI is negatively charged, consistent with the ability of IRI to bind to the anion-exchange column (Figure 2C).

Quantification of IRI in Cerebellum. IRI was purified from whole cerebellum by the four-step procedure described above. To quantitate the activity of IRI at each stage of the purification, we developed a standard assay for measuring IRI activity. Typical inhibition curves for calculating the amount of IRI in various fractions are shown in Figure 8. Curve-fitting analyses were used to calculate the volume of IRI needed for one inhibitory unit in a given fraction, which was then used to calculate the number of inhibitory units in that fraction.

Table 1: Purification of IRI from Canine Cerebellum

		activity (inhibitory units)	
step[a]	mg protein	total	per equivalent of aldehyde
Hom	73	75K	0.02
Ex	4	54K	
GF1	0.1	35K	
GF2	0.03	15K	
MQ	(0)	12K	4.5

[a] Hom = cerebellar homogenate; Ex = aqueous phase of Folch extract of Hom; GF1 = gel filtration of Ex (6500 Da fraction); GF2 = desalting of GF1 6500 Da fraction by gel filtration; MQ = MonoQ fractionation of GF2 (0.65 M formate eluate). See text for details.

As shown in Table 1, the first step (Folch extraction) eliminated 95% of the protein (which aggregated at the interface between the organic and aqueous phases). Gel filtration removed 97.5% of the remaining protein while recovering 64% of the applied inhibitory activity (with peak inhibitory activity in fractions 15 and 16, similar to that seen for the cerebellar microsomes). Fractions 15 and 16 were pooled and subjected to a second gel filtration (in the absence of salt), which resulted in further loss of protein and inhibitory activity (Table 1). Peak inhibitory fractions from the latter gel filtration were then subjected to anion-exchange chromatography (on a MonoQ column), which essentially eliminated the residual protein, with the majority of the applied activity eluting at 0.65 M ammonium formate (Table 1). As a first approximation of the glycan component of IRI, we utilized a glycoprotein carbohydrate estimation kit from Pierce (which uses periodate to generate aldehydes, which are then detected with a proprietary colorimetric detection reagent). Data in column 4 of Table 1 are expressed in terms of glucose equivalents, where 1 equivalent is equal to the amount of aldehyde generated from one nanomole of glucose. Table 1 also shows the amount of aldehydes for the starting material (cerebellar homogenate). Unfortunately, this aldehyde detection assay was sensitive to contamination by Tris buffer, complicating quantification of the gel-filtration fractions (which contained 20−50 mM Tris). There was no apparent reactivity, however, with ammonium formate (used in the elution of IRI from the MonoQ column).

Distribution of IRI among Neuronal and Peripheral Cells. Although IRI was originally isolated from canine cerebellum, efforts have been made to assess the presence of IRI in other tissues and cell types. In Figure 9, IRI was isolated from equivalent amounts of canine cerebellum and canine aorta to facilitate comparison of the relative abundance of IRI in these two tissues. Both tissues were homogenized and then subjected to Folch extraction, followed by gel filtration of the aqueous extract. As shown in Figure 9A, a peak of inhibitory activity was evident in fractions 15−16 (ca. 6500 Da), characteristic of IRI. By contrast, there was no inhibitory peak in the aortic preparation (Figure 9B), indicating that the level of IRI in cerebellum is substantially higher than that in aorta.

We hypothesized that IRI was preferentially distributed among neurons, and so assessed the relative amount of IRI in the neuronal cell line N1E115. As shown in Figure 9C, we did identify IRI in neuroblastoma cells (with characteristic peak inhibitory activity in a 6500 Da fraction). The amount of IRI present in neuroblastoma cells, however, is consider-

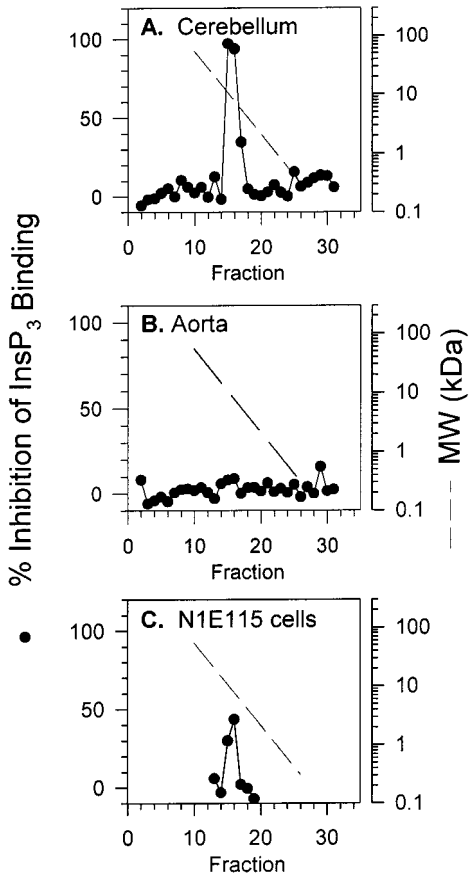

FIGURE 9: Cerebellum (A) and aorta (B) differ markedly in terms of the level of IRI. Both tissues were homogenized, and then IRI was isolated from equal amounts of homogenate (15 mg) by a combination of Folch extraction (aqueous phase) and gel filtration. IRI was present in fractions 15−16 (ca. 6500 Da) of the cerebellar preparation (panel A), but was below detection in the aortic preparation (panel B). IRI was also present in neuroblastoma cells (fractions 15−16; panel C), suggesting a neuronal distribution of IRI.

ably less than that in cerebellum. In N1E115 cells, for example, we calculate 1.7 units of IRI/μL of intracellular volume, whereas in cerebellum, we estimate the presence of 19 units/μL of intracellular volume. We have directly measured the intracellular volume in N1E115 cells using radiochemical techniques, whereas the intracellular volume of the cerebellum was estimated to be 0.49 μL/mg of wet weight (assuming 30% extracellular space, 0.7 mL of intracellular space/g of cellular weight, and homogeneous distribution of IRI among all cells of the cerebellum). The difference in IRI concentration between cerebellar cells and N1E115 cells could be greater, however, if IRI is not distributed equally among all cells of the cerebellum but is instead preferentially located in cerebellar neurons.

Comparison of IRI with Other Inhibitors of $InsP_3$ Binding. It has recently been suggested that phosphatidylinositol 4,5-bisphosphate (PIP_2) competitively inhibits $InsP_3$ binding (*31*). Lipids such as PIP_2, however, are typically extracted into the organic phase of a Folch extract, and as shown in Figure 10A, the inhibitory activity of PIP_2 is lost from the aqueous phase following Folch extraction. This contrasts with IRI, which partitions into the aqueous phase following Folch extraction (cf. Figure 2).

Calmodulin has been reported to exert effects on both $InsP_3$ binding (*19*, *32*) and Ca-dependent inhibition of the $InsP_3$-gated channel (*21*−*23*), though the effect of calmodulin on $InsP_3$ binding has been reported to be pH-sensitive (*19*, *32*). Consistent with the latter reports, concentrations of calmodulin as high as 10 μM were without effect on $InsP_3$ binding to the $InsP_3$ receptor under standard (pH 8) $InsP_3$ binding conditions (Figure 10A). At pH 7 (Figure 10B), calmodulin did inhibit $InsP_3$ binding, though the extent of inhibition was small (even in the presence of 20 μM calmodulin). IRI, on the other hand, was able to inhibit 93−100% of the $InsP_3$ binding to the cerebellar $InsP_3$ receptor at both pH 8 (Figure 8) and pH 7 (Figure 10A).

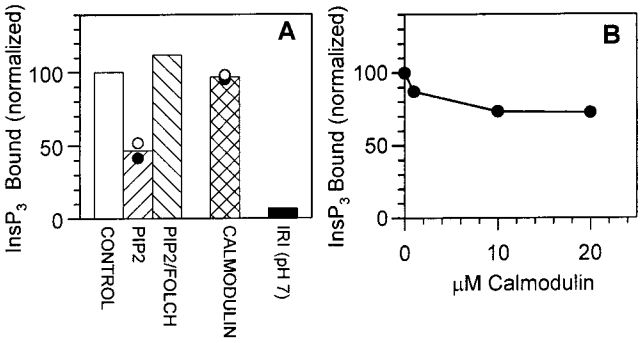

FIGURE 10: Comparison of IRI with known inhibitors of the $InsP_3$ receptor. (A) PIP_2 (10 nM) inhibited $InsP_3$ binding to the purified $InsP_3$ receptor (first hatched bar, //), but this inhibitory effect was lost from the aqueous phase upon Folch extraction (second hatched bar, \\). Calmodulin (10 μM; crosshatched bar) was without effect on $InsP_3$ binding under this standard assay condition (pH 8; see text). At pH 7, calmodulin partially inhibited $InsP_3$ binding to the purified cerebellar $InsP_3$ receptor (panel B), whereas 3 μL of IRI reduced $InsP_3$ binding to 7% ± 0.3% of the control value (mean ± SE; $n = 3$; solid bar in panel A).

DISCUSSION

The present study shows that cerebellum contains a competitive inhibitor of the $InsP_3$ receptor. Initially, we isolated this $InsP_3$ receptor inhibitor (IRI) from cerebellar microsomes and demonstrated that IRI could be separated from the $InsP_3$ receptor by heparin−Sepharose chromatography, a technique used for the purification of the $InsP_3$ receptor (*15*, *16*). Subsequently, we identified a means of removing 95% of the contaminating protein in a single step (i.e., Folch extraction), and since IRI appeared to be water-soluble, we could avoid the use of detergents (which often complicate structural and functional analyses).

The identity of IRI has yet to be determined, though our data strongly suggest that it is a sulfated glycan. Moreover, sulfo esters on IRI appear to be critical for its inhibitory activity. This contrasts with heparin, which typically requires N-linked sulfates for the inhibition of $InsP_3$ binding (*30*). IRI also differs from heparin in that IRI appears to lack a free reducing terminus. Evidence for the presence of carbohydrates in IRI comes from several experiments, including the binding of IRI by conA beads (suggesting the presence of mannose residues), preliminary thin-layer chromatography studies, and periodate assays. A negative charge on IRI was also inferred from the elution profile of IRI on the MonoQ column, the apparent presence of critical sulfo esters on IRI, and requirement for negative-ion mode for MALDI-MS analysis of IRI.

The possibility that IRI is a glycoprotein seems unlikely, since there was little or no detectable protein in a highly

purified preparation (Table 1), and IRI appeared to be insensitive to treatment with TCA or proteases. The possibility that IRI is a glycopeptide (that escaped detection by the protein assay), however, cannot be ruled out at this time. Recent studies indicate that glycopeptides can be secreted from the endoplasmic reticulum into the cytoplasm in mammalian cells (*33*).

With regard to the molecular mass of IRI, gel-filtration analyses suggest an average molecular weight of 6500 Da, though this may reflect an aggregate (tetramer) of a smaller inhibitor (1500 Da). MALDI-MS analyses showed a prominent peak at 1635 *m*/*z*, which is consistent with the predicted monomeric molecular weight (1500) based on gel filtration (Figure 2D). The ability to detect inhibitory activity in both the 6500 Da fraction and the 1500 Da fraction (Figure 2D) indicates that both the monomer and apparent tetramer are active, though it is not clear at this time if one form is more potent than the other.

Although IRI was initially isolated from cerebellar microsomes, we hypothesized that IRI may be preferentially distributed in the cytoplasm of neurons, where it acts as a competitive inhibitor of $InsP_3$ binding, and thus may explain the low $InsP_3$ sensitivity of Ca release in neurons such as the cerebellar Purkinje cell (*11*) and neuroblastoma cells (*14*). Consistent with this hypothesis, preliminary studies of IRI did show a predominance of IRI in a cytoplasmic fraction of cerebellum (compared to microsomes) when normalized to the amount of starting material. This apparent distribution, however, may be subject to the conditions used in the isolation, as a high ionic strength buffer (typically used in the preparation of microsomes) reverses the inhibitory effect of IRI, probably by promoting the dissociation of IRI from the microsomes (Figure 3).

If IRI does contribute to the low $InsP_3$ sensitivity of Ca release in neurons such as the cerebellar Purkinje cell and neuroblastoma cells, then the level of IRI should be higher than that in peripheral tissues, which typically exhibit a high sensitivity to $InsP_3$. Efforts were therefore made to quantitate IRI in cerebellum and to compare this level with that in a peripheral tissue (e.g., aorta), which contains both endothelial cells and smooth muscle cells known to exhibit a high sensitivity to $InsP_3$-induced Ca release (*11*, *34*, *35*). IRI could not be detected in the aortic extract, whereas IRI was abundant in an equivalent weight of cerebellum. To further test the correlation between level of IRI and $InsP_3$ sensitivity of a tissue, we extracted IRI from a neuronal cell line known to have an intermediate sensitivity to $InsP_3$. That is, the neuronal cell line N1E115 has been shown to exhibit half-maximal $InsP_3$-induced Ca release at 1−2 μM $InsP_3$ (*14*), which is approximately 10 times higher than that seen in peripheral tissues (*11*) or an aortic smooth muscle line (*34*) (i.e., 0.1−0.2 μM). Furthermore, this value for N1E115 cells (1−2 μM $InsP_3$) is considerably less than that reported for cerebellar Purkinje cells (*11*), where $InsP_3$-induced Ca release begins at 9 μM and continues to increase up to 80 μM $InsP_3$. Thus, if IRI concentration is inversely correlated with $InsP_3$ sensitivity of Ca release, one might expect a 10-fold lower concentration of IRI in the N1E115 cells than in the cerebellum. On the basis of the recovery of IRI from cerebellum and N1E115 cells, we estimate that N1E115 cells contain 1.7 units of IRI activity/μL of intracellular volume, whereas cerebellum is estimated to contain 19 units of IRI activity/μL of intracellular volume. These results are thus consistent with the hypothesis that elevated levels of IRI in neuronal cells may explain the low $InsP_3$ sensitivity of $InsP_3$-induced Ca release.

It should be noted that the actual amount of IRI isolated from these tissues/cells is very small (in fact, there was no visible pellet in the MonoQ eluate upon lyophilization). Preliminary calculations (based on a periodate assay) suggests that the intracellular concentration of IRI may be approximately 3 μM in cerebellum, though further analyses are needed in this regard. Moreover, this calculation assumes an equal distribution of IRI throughout all cells of the cerebellum, which would be expected to lead to an underestimation of the IRI concentration [since nonneuronal cells such as astrocytes exhibit a high sensitivity to $InsP_3$ (*11*) and thus would not be expected to contain IRI].

It has recently been proposed that the phospholipid phosphatidyl inositol 4,5-bisphosphate (PIP_2) acts as a competitive inhibitor of $InsP_3$ binding (*31*), but IRI is clearly distinct from PIP_2, as described in the Results section. It has also been suggested that calmodulin can inhibit $InsP_3$ binding (*19*, *32*), though IRI is also distinct from calmodulin. Moreover, our studies indicate that calmodulin is a weak inhibitor of $InsP_3$ binding compared to IRI. A recent study has also suggested that brain cytosol contains a glycoprotein (molecular weight in excess of 300 kDa) that inhibits $InsP_3$ binding. Although we detected a small amount of high molecular weight inhibitor in our isolation procedures (see Figure 1), the predominant inhibition of $InsP_3$ binding in our studies was observed in a gel-filtration fraction of 6500 Da. The inability of the previous study (*36*) to detect IRI in brain cytosol probably reflects their use of a dialysis membrane (25 kDa cutoff) in the purification procedure. That is, IRI (6500 Da or less) would be lost during the dialysis step.

The presence of an endogenous competitive inhibitor in neuronal tissues may be important for extending the dynamic range of the $InsP_3$-gated Ca channel and thus allowing a graded response to multiple synaptic inputs. The cerebellar Purkinje cell, for example, plays a key role in motor learning and receives input from numerous climbing fibers and parallel fibers, which can promote long-term depression (a form of synaptic plasticity/learning). $InsP_3$-induced Ca release plays a key role in the development of long-term depression (*6*−*8*), raising the possibility that a low $InsP_3$ sensitivity of neurons such as the cerebellar Purkinje cell may delay the onset of long-term depression (i.e., requiring multiple synaptic inputs from parallel fibers). As $InsP_3$ is a global intracellular second messenger (diffusing rapidly throughout the cell), a low $InsP_3$ sensitivity of neurons may also contribute to the recently described local Ca signaling (*37*, *38*) at the site of synaptic stimulation, which may be important for the generation of local areas of long-term depression in a given neuron.

In summary, the present study provides evidence for a novel, endogenous inhibitor of $InsP_3$ binding (IRI) in neuronal cells. IRI appears to be a sulfated glycan (ca. 1635 Da), whose inhibitory activity is dependent on the presence of sulfo ester group(s). Moreover, the distribution of IRI among cell types suggests that IRI may be an important determinant of the low $InsP_3$ sensitivity of neurons, and thus may contribute to setting the threshold for the development

of long-term depression (learning) in neurons such as the cerebellar Purkinje cell.

ACKNOWLEDGMENT

The expert technical assistance of Dr. S. Syrbu is gratefully appreciated. Drs. L. Loew, B. E. Ehrlich, A. Fein, C. Fink, R. Berlin, P. Campagnola, T. Hla, L. Jaffe, and R. Sha'afi are gratefully acknowledged for valuable discussions during the preparation of the manuscript.

REFERENCES

1. Ross, C. A., Danoff, S. K., Schell, M. J., Snyder, S. H., and Ullrich, A. (1992) *Proc. Natl. Acad. Sci. U.S.A. 89*, 4265−4269.
2. De Smedt, H., Missiaen, L., Parys, J. B., Bootman, M. D., Mertens, L., Van Den Bosch, L., and Casteels, R. (1994) *J. Biol. Chem. 269*, 21691−8.
3. Newton, C. L., Mignery, G. A., and Sudhof, T. C. (1994) *J. Biol. Chem. 269*, 28613−9.
4. Clapham, D. E. (1995) *Cell 80*, 259−68.
5. Berridge, M. J. (1993) *Nature 361*, 315−325.
6. Khodakhah, K., and Armstrong, C. M. (1997) *Proc. Natl. Acad. Sci. U.S.A. 94*, 14009−14.
7. Kasono, K., and Hirano, T. (1995) *Neuroreport 6*, 569−72.
8. Inoue, T., Kato, K., Kohda, K., and Mikoshiba, K. (1998) *J. Neurosci. 18*, 5366−73.
9. Kano, M., and Kato, M. (1987) *Nature 325*, 276−9.
10. Ogden, D. C., Khodakhah, K., Carter, T. D., Gray, P. T., and Capiod, T. (1993) *J. Exp. Biol. 184*, 105−27.
11. Khodakhah, K., and Ogden, D. (1993) *Proc. Natl. Acad. Sci. U.S.A. 90*, 4976−80.
12. Carter, T. D., and Ogden, D. (1992) *Proc. R. Soc. London, B: Biol. Sci. 250*, 235−41.
13. Watras, J., Bezprozvanny, I., and Ehrlich, B. E. (1991) *J. Neurosci. 11*, 3239−3245.
14. Fink, C. C., Slepchenko, B., Moraru, I. I., Schaff, J., Watras, J., and Loew, L. M. (1999) *J. Cell Biol. 147*, 929−36.
15. Supattapone, S., Worley, P. F., Baraban, J. M., and Snyder, S. H. (1988) *J. Biol. Chem. 263*, 1530−4.
16. Maeda, N., Niinobe, M., and Mikoshiba, K. (1990) *EMBO J. 9*, 61−7.
17. Furuichi, T., Yoshikawa, S., Miyawaki, A., Wada, K., Maeda, N., and Mikoshiba, K. (1989) *Nature 342*, 32−8.
18. Marks, A. R., Tempst, P., Chadwick, C. C., Riviere, L., Fleischer, S., and Nadal-Ginard, B. (1990) *J. Biol. Chem. 265*, 20719−22.
19. Patel, S., Morris, S. A., Adkins, C. E., O'Beirne, G., and Taylor, C. W. (1997) *Proc. Natl. Acad. Sci. U.S.A. 94*, 11627−32.
20. Yamada, M., Miyawaki, A., Saito, K., Nakajima, T., Yamamoto-Hino, M., Ryo, Y., Furuichi, T., and Mikoshiba, K. (1995) *Biochem. J. 308*, 83−8.
21. Missiaen, L., Parys, J. B., Weidema, A. F., Sipma, H., Vanlingen, S., De Smet, P., Callewaert, G., and De Smedt, H. (1999) *J. Biol. Chem. 274*, 13748−51.
22. Hirota, J., Michikawa, T., Natsume, T., Furuichi, T., and Mikoshiba, K. (1999) *FEBS Lett. 456*, 322−6.
23. Michikawa, T., Hirota, J., Kawano, S., Hiraoka, M., Yamada, M., Furuichi, T., and Mikoshiba, K. (1999) *Neuron 23*, 799−808.
24. Watras, J., Syrbu, S., and Ehrlich, B. E. (1999) *Biophys. J. 76*, A375.
25. Folch, J., Lees, M., and Stanely, G. H. S. (1957) *J. Biol. Chem. 226*, 497−509.
26. Bradford, M. M. (1976) *Anal. Biochem. 72*, 248−54.
27. Benevolensky, D., Moraru, I., and Watras, J. (1994) *Biochem. J. 299*, 631−636.
28. Fink, C., Morgan, F., and Loew, L. M. (1998) *Biophys. J. 75*, 1648−58.
29. Bligh, E. G., and Dyer, W. J. (1959) *Can. J. Biochem. Physiol. 37*, 911−917.
30. Ghosh, T. K., Eis, P. S., Mullaney, J. M., Ebert, C. L., and Gill, D. L. (1988) *J. Biol. Chem. 263*, 11075−11079.
31. Lupu, V. D., Kaznacheyeva, E., Krishna, U. M., Falck, J. R., and Bezprozvanny, I. (1998) *J. Biol. Chem. 273*, 14067−70.
32. Sipma, H., De Smet, P., Sienaert, I., Vanlingen, S., Missiaen, L., Parys, J. B., and De Smedt, H. (1999) *J. Biol. Chem. 274*, 12157−62.
33. Romisch, K., and Ali, B. R. S. (1997) *Proc. Natl. Acad. Sci. U.S.A. 94*, 6730−4.
34. Fink, C. C., Slepchenko, B., and Loew, L. M. (1999) *Biophys. J. 77*, 617−28.
35. Missiaen, L., De Smedt, H., Parys, J. B., Sienaert, I., Valingen, S., and Casteels, R. (1996) *J. Biol. Chem. 271*, 12287−93.
36. Hirata, M., Yoshida, M., Kanematsu, T., and Takeuchi, H. (1999) *Mol. Cell. Biochem. 190*, 179−84.
37. Finch, E. A., and Augustine, G. J. (1998) *Nature 396*, 753−6.
38. Takechi, H., Eilers, J., and Konnerth, A. (1998) *Nature 396*, 757−60.

BI992175V